Transient Dynamics of Airflow near a Local Heat Source

Y. L. LIN* AND R. B. SMITH

Department of Geology and Geophysics, Yale University, New Haven, CT 06511

(Manuscript received 12 September 1984, in final form 12 July 1985)

ABSTRACT

The response of a stratified atmosphere to local heating is a common element in several problems in mesoscale dynamics. To investigate this response, a time-dependent linearized problem is solved analytically for an elevated, local heat source turned on as a pulse in a stratified, moving fluid. The thermally induced circulation in the vicinity of the drifting disturbance is qualitatively similar to that of a cumulus cloud in mean wind. The updraft at the center of this cloud is surrounded by the compensating downdrafts at early times, even if that air has also been heated. Once the updraft at the drifting center weakens, upward motion begins in the adjacent regions. An integration of the pulse solution yields the response to steady heating, turned on at $t = 0$. As steady state is approached, this solution exhibits a region of positive displacement moving downstream while negative displacements develop near the stationary heat source. The solution offers an explanation to a curious negative phase relationship between heating and displacement and the lack of a true steady state noted by other authors. It is suggested that the nature of this response may help to explain three problems in mesoscale dynamics: cloud interaction, heat island/orographic rain, and the squall line.

1. Introduction

There are a number of problems in mesoscale dynamics which are related to the response of a stably stratified fluid to local heating. A few of these, including steady and unsteady examples, are mentioned below to motivate a discussion of the dynamics of this response. In a study of the upslope orographic rain problem, Smith and Lin (1982, denoted as SL) found that the phase relationship between the heating and the induced vertical displacement is negative in a moving airstream. That is, air descent is established just upstream of the prescribed heated regions so that negative vertical displacements dominate in the heated regions. This is consistent with other studies of the orographic rain problem (e.g., Fraser et al., 1973; Barcilon et al., 1980) in which it was found that mountain waves are weakened by the latent heating. This is so because in a marginally saturated atmosphere, the latent heating tends to be located in regions of positive displacement. This is also consistent with the study by Raymond (1972) of airflow over a ridge with low-level sensible heating and cooling. Raymond found that mountain waves were weakened by heating and strengthened by cooling.

This kind of process is also relevant to flow past heated islands at sea or urban "heat islands." The observations over heat islands such as Anegada (Malkus, 1963) and Barbados (DeSouza, 1972; summarized in Garstang et al., 1975) show that there is a region of descent over the heated island followed by an ascent over the ocean on the downwind side. One theoretical result that disagrees with this (by predicting in phase vertical displacement and heating) is Malkus and Stern (1953). As pointed out by Olfe and Lee (1971) and SL, this is because of an incorrect upper boundary condition. The energy argument in section 3 below, explains how an incorrect radiation condition aloft would reverse the displacement in the heating region. The relationship between heating and vertical motion also arises in the study of thunderstorm drafts. Thorpe et al. (1980) found that an upward motion is produced near a stationary heat sink in the "jump" type of flow associated with thunderstorm downdrafts. Again this may seem to disagree with intuition but is consistent with the above phenomena.

Mesoscale problems of thermal or mechanical forcing cannot be fully understood using a steady state model. The importance of solving a time-dependent problem has been demonstrated in the studies of mountain waves (e.g., Hoiland, 1951; Palm, 1953; Queney, 1954), which provide insight into how a forced perturbation is established when the wind becomes practically steady over a mountain terrain. The transient heat island problem has been treated by Smith (1957), but without a full discussion of the energetics and the problematic approach to steady state. Unsteady problems with thermal forcing have also been investigated in other contexts. The internal gravity waves generated by local prescribed heating have been investigated by Blumen and Hendl (1969) with application to Joule heating in the ionosphere. This paper was quite

* Present affiliation: Department of Physics and Atmospheric Science, Drexel University, Philadelphia, PA 19104.

general in that compressibility was partially accounted for with the anelastic approximation and the disturbance was not required to be hydrostatic. On the other hand, only the wave energy flux, not the disturbance fields themselves, was computed and there was a minor error in the interpretation of this flux. The vertical energy flux $\overline{p'w'}$ was assumed to be related to the total heating so that the difference was attributed to horizontal energy flux. Actually these two quantities cannot be directly compared as they are of different order in the amplitude of the heating. This can be seen by taking a large heating so that the "flux" exceeds the heat input or by taking a combined heating-cooling so that the net heating is zero while the energy flux remains nonzero. It is the second-order heating work that must balance the energy flux divergence. A related point is that in an unstructured atmosphere with no wave trapping (such as in Blumen and Hendl and the present work), a pair of infinite horizontal planes placed above and below the wave source will intercept all the wave energy—no additional horizontal energy flux need be considered.

The mathematical problem of wave generation by local thermal source also arises in the study of large explosions (e.g., Pekeris, 1948; Scorer, 1950; Hunt et al., 1960; Weston, 1962). These papers, however, are primarily concerned with the far field radiation of acoustic-gravity waves.

To begin this study, a solution will be obtained to the problem of adding heat as a pulse to a moving stratified fluid. A similar case with a narrow impulse of mass source aloft in a quiescent atmosphere has been considered by Raymond (1983) in a study of Wave-CISK mechanism. Our solution, however, will be somewhat more general as it allows a heating distribution of finite width and height and includes the advection effect of a constant mean wind. This will allow us to investigate the flow behavior near the heat source as well as the interaction with the mean wind. The solution to pulse heating will then be extended to approach stationary heating. The negative relationship of the steady heating and the induced vertical displacement which then emerges can be explored more fully. The thermally induced gravity wave and the vertical transport of horizontal momentum will be discussed. Finally, the solutions are applied to a variety of mesoscale problems of diabatic flow such as the cloud interaction, heat island/upslope orographic rain, and squall line. Even though the solutions are limited to an atmosphere with simple structure such as constant stability and mean wind, it still provides considerable insight into the dynamics of general diabatic flows in the atmosphere.

2. The governing equations and a solution with pulse heating

Consider a two-dimensional, inviscid, nonrotating, hydrostatic, low Mach number flow where the perturbations from a background horizontal flow are small. The governing equation for the vertical velocity can be written as (also see SL)

$$\left(\frac{\partial}{\partial t} + U\frac{\partial}{\partial x}\right)^2 w_{zz} + N^2 w_{xx} = \frac{g}{c_p\bar{T}} q_{xx} \quad (1)$$

where N is the buoyancy frequency and U is the incoming flow, both assumed to be independent of height, and q is a heating rate per unit mass. Other symbol definitions can be found in SL. The hydrostatic assumption will be valid for waves generated by a mesoscale heat source or a mountain having intrinsic frequency small compared to the buoyancy frequency. If the local time derivative in the above equation is removed, the equation reduces to that studied in SL. To solve the above equation, we determine the relevant Green's function. Taking the Fourier transform in $x(x \rightarrow k)$ and Laplace transform in $t(t \rightarrow s)$ of Eq. (1), we have

$$\hat{w}_{zz} + \lambda^2\hat{w} = \frac{g\lambda^2}{c_p\bar{T}N^2}\hat{q}, \quad (2)$$

where $\lambda \equiv iNk/(s + iUk)$ and $\mathrm{Re}(s) > 0$.

We do not transform in z so that the method used here can be extended to a structured atmosphere. We shall examine two extreme cases of pulse and steady heating functions. First, let us consider a simple case of a pulse of heat in an unbounded fluid:

$$q(t, x, z) = Q_0\delta(t)\left(\frac{b^2}{x^2 + b^2}\right)\delta(z), \quad (3)$$

where δ is the Dirac delta function, Q_0 is the amplitude of the heating and b the half-width of the heat source. Taking the Fourier and Laplace transforms of (3) and inserting it into Eq. (2) gives

$$\hat{w}_{zz} + \lambda^2\hat{w} = \frac{gQ_0b}{c_p\bar{T}N^2}\lambda^2 e^{-bk}\delta(z). \quad (4)$$

Integrating Eq. (4) from $z = 0^-$ to 0^+ twice gives us two interface conditions. An appropriate set of upper and lower boundary conditions for an unbounded fluid are the radiation conditions, i.e., $\hat{w} \sim \exp(i\lambda|z|)$ as $|z| \rightarrow \infty$. Thus the solution of Eq. (4) can be obtained

$$\hat{w}(s, k, z) = \frac{-igQ_0b}{2c_p\bar{T}N^2}\lambda e^{-kb}e^{i\lambda|z|}. \quad (5)$$

The above solution decays at infinity because $\mathrm{Re}(s) > 0$. The vertical displacement, η, defined by $w \equiv D\eta/Dt$, may be written as

$$\hat{\eta}(s, k, z) = \frac{gQ_0bke^{-kb}}{2c_p\bar{T}N(s + iUk)^2}\exp\left(-\frac{Nk|z|}{s + iUk}\right). \quad (6)$$

The inverse Laplace and Fourier transforms of the above equation can then be performed giving

$$\eta(t, x, z) = \frac{gbQ_0 t}{2c_p\bar{T}N(b^2 + X^2)^2} \exp\left(-\frac{Nbt|z|}{b^2 + X^2}\right)$$
$$\times \left[(b^2 - X^2)\cos\left(\frac{NtX|z|}{b^2 + X^2}\right) + 2bX \sin\left(\frac{NtX|z|}{b^2 + X^2}\right)\right], \quad (7)$$

where $X = Ut - x$. The solution for a more realistic shape of the heating functions in the vertical can be obtained by use of Green's function method. We also generalize (7) to include a rigid lower boundary using the method of images. The vertical displacement for a pulse heating distributed uniformly in a layer from $z_0 - d$ to $z_0 + d$ in a half plane can be written as

$$\begin{aligned}\eta(t, x, z) = {} & [A/N(b^2 + X^2)]\langle 2b[H(z_0 - d) \\ & - H(z_0 + d)] + \mathrm{sgn}(z - z_0 - d) \\ & \times e^{-bB|z-z_0-d|}[X \sin(BX|z - z_0 - d|) \\ & + b\cos(BX|z - z_0 - d|)] - \mathrm{sgn}(z - z_0 + d) \\ & \times e^{-bB|z-z_0+d|}[X \sin(BX|z - z_0 + d|) \\ & + b\cos(BX|z - z_0 + d|)] + e^{-bB(z+z_0+d)} \\ & \times \{X \sin[BX(z + z_0 + d)] + b\cos[BX \\ & \times (z + z_0 + d)]\} - e^{-bB(z+z_0-d)}\{X \sin[BX \\ & \times (z + z_0 - d)] + b\cos[BX(z + z_0 - d)]\}\rangle \quad (8)\end{aligned}$$

where

$$A = \frac{gbQ_0}{2c_p\bar{T}N}, \quad B = \frac{Nt}{b^2 + X^2}, \quad X = Ut - x.$$

The symbols H and sgn denote the step function and the sign function, respectively. This formula (8) is an extension of the result of Raymond (1983) as it allows a heating distribution of finite width and height (i.e., b and d) and includes the advection effect of a constant mean wind.

The vertical displacements in an unbounded atmosphere produced by a layer of heat source which is active at $t = 0$ only, are shown in Fig. 1. The solution is given by Eq. (8) after excluding the last two terms, which are the effects of wave reflection from the lower boundary. The response of the fluid to heating has the form of a region of mostly upward displacements drifting with the mean wind. The most strongly heated air rises monotonically, approaching a new level. Less strongly heated air just to the left and right, sinks initially before finally rising to a new level. The initial sinking is caused by a downdraft associated with the updraft at the center. Still further away from the drifting center, the displacement is best described as a symmetric field of weak dispersing gravity waves. The drifting region leaves the right boundary of the domain shown in the figure at about 10 000 seconds. Conceptually, the drifting disturbance is similar to an isolated

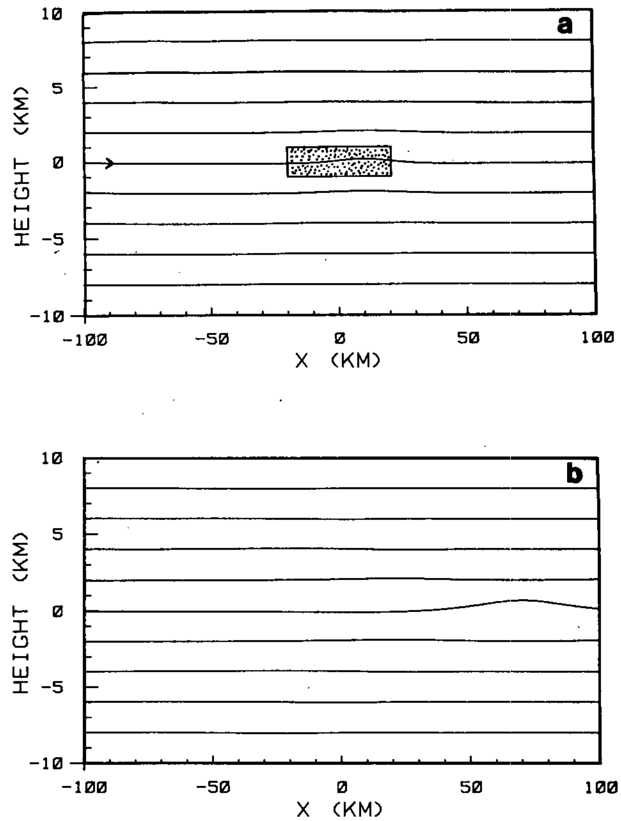

FIG. 1. Vertical displacement of the hydraulic flow in an unbounded fluid with a heat source applied at $t = 0$ s as a pulse. The stippled region shows the region of strongest heating but not the wings of the bell-shaped function (3). The basic flow is directed from left to right. This solution is given by Eq. (8), excluding the lower boundary reflections, with $U = 10$ m s^{-1}, $N = 0.01$ s^{-1}, $\bar{T} = 273$ K, $Q_0 = 2000$ J kg^{-1}, $b = 20$ km, and $d = 1$ km. Two times are shown in (a) 1000 s, and (b) 7000 s. The actual top, bottom, and lateral boundaries are at infinity.

cumulus cloud produced by a single pulse of latent heat released during a brief period of condensation.

Still considering the unbounded case, the vertical displacement at the center of the heated layer, $z = 0$, can be written [from (8)]

$$\hat{\eta} = \left(\frac{1}{1 + \hat{x}^2}\right)\left\{1 - \exp\left(-\frac{\hat{t}}{1 + \hat{x}^2}\right)\right.$$
$$\left.\times \left[\hat{x}\sin\left(\frac{\hat{t}\hat{x}}{1 + \hat{x}^2}\right) + \cos\left(\frac{\hat{t}\hat{x}}{1 + \hat{x}^2}\right)\right]\right\}, \quad (9)$$

where $\hat{x} = (x - Ut)/b$, $\hat{t} = Ndt/b$, and $\hat{\eta} = \eta(x, 0, t)c_p\bar{T}N^2/gQ_0$. There are two regions of interest: 1) the region of the drifting heated air and 2) the region of the initial heating. To investigate the behavior around the center of drifting disturbance, the reference frame is moved with the mean wind (Fig. 2a). The curves at different times represent the vertical displacements at different locations downstream. The early response of the fluid to the heating is an upward displacement at

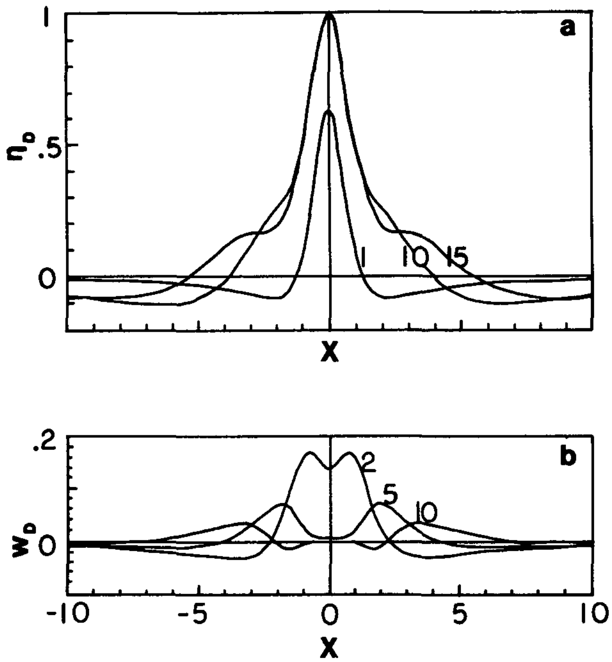

FIG. 2. (a) The vertical displacement at the center level of the pulse heat source in a frame moving with the basic wind. The solution is given by Eq. (9). The four curves represent $\hat\eta$ at $\hat t$ = 1, 5, 10 and 15. Notice that (1) there is a strong updraft around the drifting center, and (2) there are two regions of downdrafts to the sides of the growing cloud. (b) The vertical velocity corresponding to (a) at $\hat t$ = 1 and 5.

the drifting center and downward displacements to the upwind and downwind sides of the growing disturbance. The weak downward displacements are necessary for compensating the upward motion at the center as required by the continuity equation even though that air was also heated by the wings of the pulse. Once the updraft at the drifting center weakens, the fluid in the adjacent regions can rise. The displacement at the drifting center ($X = 0$) grows as $[1 - \exp(-\hat t)]$. The final displacement $\hat\eta(\infty, x, z)$ is everywhere proportional to the total amount of heat received by that air parcel. This is true provided only that the temperature anomalies approach zero for large time. For the pulse heating problem this "parcel argument" gives [from (3)]

$$\hat\eta(\infty, x, z) = \frac{1}{1+\hat x^2} \quad \text{for } z_0 - d < z < z_0 + d \qquad (10)$$

and zero elsewhere. This agrees with (9) as $\hat t \to \infty$.

Figure 2b shows the nondimensional vertical velocity which corresponds to Fig. 2a. This is obtained by taking the time derivative of Eq. (9):

$$\hat w_D = \frac{1}{(1+\hat x^2)^2}\exp\left(\frac{-\hat t}{1+\hat x^2}\right) \times \left[2\hat x \sin\left(\frac{\hat t\hat x}{1+\hat x^2}\right) + (1-\hat x^2)\cos\left(\frac{\hat t\hat x}{1+\hat x^2}\right)\right]. \qquad (11)$$

The updraft at the drifting center is accompanied by downdrafts on both sides in the earlier stages. At later times, such as for $\hat t = 2$, there are two updrafts developed, which will propagate outward. Those updrafts will overcome the downward displacement produced earlier and generate upward displacement at later times, as can be seen from Fig. 2a. At this time, the original disturbance has split into two.

Consider now the flow behavior at the origin of the initial heating. The solution can be obtained by setting $x = 0$ in $\hat x$ in (9), the nondimensional form reduces to

$$\hat\eta_0 = \frac{1}{1+\hat t^2}\left\{1 - \exp\left(-\frac{\hat t}{F(1+\hat t^2)}\right) \times \left[\hat t \sin\left(\frac{\hat t^2}{F(1+\hat t^2)}\right) + \cos\left(\frac{\hat t^2}{F(1+\hat t^2)}\right)\right]\right\}, \qquad (12)$$

where the nondimensional number F is defined as U/Nd. An example is shown in Fig. 3. Notice that the nondimensional number F represents a Froude number associated with the heating. A similar number has been used in a study of thunderstorm drafts by Thorpe et al. (1980). The value of $\hat\eta_0$ depends on the Froude number of the flow, and will change sign at $F = 1/\pi$, $1/2\pi$, · · · etc. For a case of a shallow heating layer, the Froude number is greater than $1/\pi$. As can be seen from Eq. (12), $\hat\eta$ decays as $\hat t^{-1}$ as $t \to \infty$ (Fig. 3). The positive vertical displacement at earlier times is produced by the updraft generated by the pulse heating. Once the growing disturbance is drifting downstream with the mean wind, it leaves a negative displacement at the heating origin because the origin is located in the downwash region of the drifting disturbance. The downward displacement reaches its extreme at about $\hat t = 3.5$ ($3.5b/U$ in dimensional time), and thereafter diminishes as the heated air drifts farther downstream. As we shall see, this downwash can produce a downward displacement near a stationary heat source as found in SL.

Before leaving the pulse heating, consider briefly the energy and momentum fluxes associated with the disturbance (a more complete discussion is included at the end of the next section). The vertical flux of horizontal momentum $\overline{u'w'}$ is zero at all times for pulse

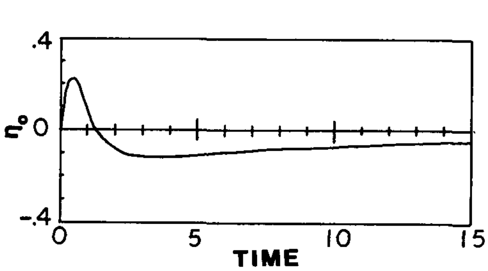

FIG. 3. The vertical displacement at the origin of the pulse heating. The solution is given by Eq. (12). Notice that the response of η_0 is an upward displacement followed by a downward displacement, as the heated air drifts away. The time and displacements are nondimensionalized.

heating due to the left-right symmetry of the problem. The vertical energy flux $\overline{p'w'}$, integrated over time, is directly related to the total heating work which is proportional to the space-time integral of $-p'q$. Pulse heating is a special case in this regard as $p' \sim \int (-q)dt$ at each point during the heating; no vertical motion having yet occurred. Thus, the heating work becomes proportional to

$$\int\int \left(q \int qdt\right) dxdz = \frac{1}{2}\int\int \left(\int qdt\right)^2 dxdz.$$

3. The approach to steady state

Previous studies of steady heating in a flowing atmosphere in connection to orographic rain (SL), heat islands (Garstang et al., 1975), and thunderstorm drafts (Thorpe et al., 1980) have noted a curious negative relationship between heating and vertical displacement. As we shall see, this result is directly related to the steadiness. To clarify these previous results and for use in later sections of this paper, we here describe the approach to steady state for heating begun at $t = 0$.

The vertical displacement for the steady state heating can be obtained by the Green's function method which amounts to integrating Eq. (8) with respect to time

$$\eta(t, x, z) = \int_0^t \eta(t - t_0, x, z)dt_0. \quad (13)$$

Figure 4 shows an example in which a heat source concentrated in the stippled region is given by a Heaviside function at $t = 0$ in an unbounded fluid. The solution is given by Eq. (13) by excluding the lower boundary reflections [i.e., the last two terms in Eq. (8)]. The integrals in Eq. (13) are computed numerically using the Simpson's rule. The response of the fluid has two quite separate parts. First, there exists a region of upward displacement generated first at the origin of the heat source and advected downstream by the mean wind. The amplitude of the displacements keeps growing with time. Notice that the peak of the upward displacement appears to advect downstream with a slower speed ($\sim 0.7U$) than the mean flow. The upward displacement is a superposition of an infinite number of individual elements corresponding to individual pulse heating separated at infinitesimal time interval. For waves growing with time, the peak of the upward displacement propagates downstream with a slower speed than the mean wind. In addition there is a downward displacement in the vicinity of the heat source, which develops at a much slower rate than that of the drifting disturbance. Associated with this downward displacement there are upward propagating waves present, with an upstream phase tilt.

One difficulty in understanding the approach to steady state is that the integral of (13) does not remain bounded as $t \rightarrow \infty$. Far downstream, this is because of the continued growth of positive displacement in the heated air. At $x = 0$, the negative displacement

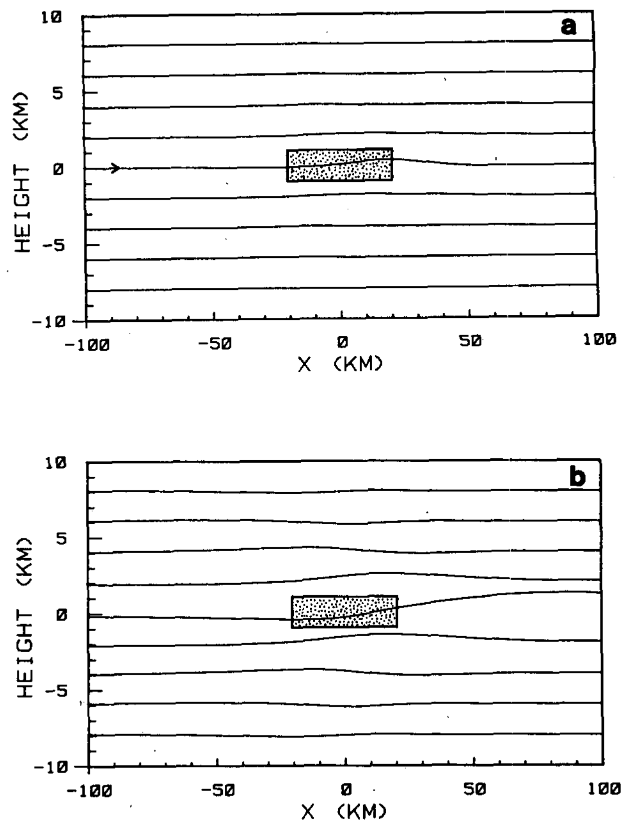

FIG. 4. Vertical displacement in the case of a stationary heat source (stippled) begun at $t = 0$. This flow is given by Eq. (13), excluding the lower boundary reflections, with $U = 10$ m s^{-1}, $N = 0.01$ s^{-1}, $\bar{T} = 273$ K, $Q_0 = 1$ J kg^{-1} s^{-1}, $b = 20$ km, $d = 1$ km, and $c = 0$ km. Two times are shown in (a) 3000 s, and (b) 7000 s.

grows slowly but continuously because of the downdraft associated with each drifting parcel of heated air. To obtain a steady state solution, as in SL, it is necessary to include a compensating, widespread cooling so that the net heating at each level is zero. The transient solutions in this paper help to clarify the necessity for this compensating cooling.

The problem of the negative phase relationship between the heating rate and the induced vertical displacement in the vicinity of the heat source, as raised in SL, can be understood through the transient approach. The response of the air parcel in the vicinity of the stationary heat source can be obtained by integrating the Green's function for the pulse heating, i.e. Eq. (12). As can be seen from Fig. 3, the vertical displacement will be negative at the heating center due to the superposition of the downdrafts associated with all the regions of heated air drifting downstream.

An alternative way to explain this phenomenon is by the energy budget. The linearized steady state energy equation is

$$\frac{\partial}{\partial x}(EU + pu) + \frac{\partial}{\partial z}(pw) = -(g^2/c_p\bar{T}N^2)pq, \quad (14)$$

where $E = \frac{1}{2}\rho[u^2 + (g\rho/N\bar{\rho})^2]$ is the wave energy. According to Eq. (14), in order to add energy to the system the steady heating must be added where the air density is low, i.e. at high temperature. This implies that the perturbation flow field must adjust itself so that the regions of negative density anomaly (negative displacement) receive the heat.

Consider now the time evolution of the momentum flux caused by an elevated heat source in a moving fluid. The vertical flux of horizontal momentum may be defined as

$$F(z) = \bar{\rho} \int_{-\infty}^{\infty} uwdx.$$

Figure 5 shows the evolution of the vertical transport of horizontal momentum corresponding to the flow field in Fig. 4. The gravity waves produced by a pulse of heat in an unsheared flow are symmetric about its center and impart no net momentum flux to the flow. However, the waves associated with the negative vertical displacement in the vicinity of a steady heat source, contribute momentum flux to the flow because of the phase tilt of the vertical displacement. There exists a layer of negative (positive) momentum flux above (below) the center level of heating layer. The magnitude of the momentum flux increases as the gravity wave associated with the steady heating becomes stronger and propagates to higher (lower) layers. In the upper layer, the downward transport of momentum flux is a consequence of the upstream phase tilt of the vertical displacement, which gives a greater horizontal perturbation velocity ($u > 0$) in the downward motion ($w < 0$). The downward (upward) transport of momentum flux in the upper (lower) layer is accompanied by an upward (downward) energy flux associated with the steady heating as mountain wave theory (Eliassen and Palm, 1960). The convergence of momentum flux at the heating level must act to accelerate the flow there (slowly, as it is a second-order quantity) while air above and below is decelerated.

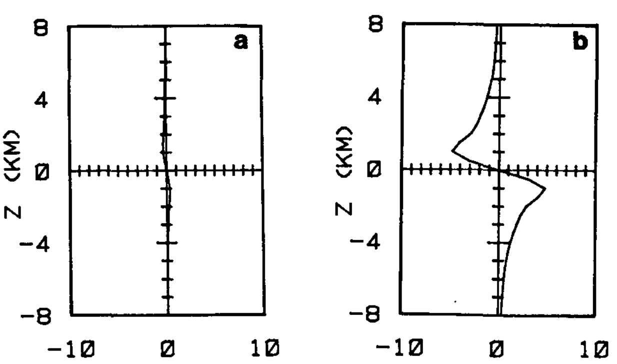

FIG. 5. The vertical transport of horizontal momentum for the flow fields in Fig. 4. The units of the momentum flux are 10^4 Newton m^{-1}.

4. Applications to problems of diabatic flow in the atmosphere

In this section we briefly discuss the applications of the foregoing dynamics to three problems.

a. Cloud interaction

It is often observed that two nearby clouds or convective elements may unite to form a single larger, taller, and more intense dynamical entity or interact in a way that a new updraft develops in the "bridge air" while the original clouds still keep their identities (e.g., Byers and Braham, 1949; Malkus, 1954; Dennis et al., 1970; summarized in Westcott, 1984). Even though the microphysical processes of cloud interaction are complicated, one might still be able to gain some insight into this using an idealized model. In the following we investigate the possibility that waves generated by latent heating in cumulus clouds might allow new clouds to form or pairs of clouds to interact.

It was shown in Fig. 2 that the response to local heating would be a decaying wave pattern moving out from the source. At the same altitude as the heating, and in an unbounded fluid, this decay is particularly rapid, as shown in Fig. 2b. In fact, considering that the heating function (3) decays gradually as $|x| \to \infty$, the waves of vertical motion do not really extend beyond the heating region. A simple explanation is that for internal gravity waves with nearly horizontal group velocity (i.e., vertical wave number) the group speed vanishes. Furthermore, in this limit, the waves induce no vertical motion.

We conclude that observed or simulated cloud interaction must arise from

1) a nearby solid boundary allowing reflection of waves which then induce vertical motion at the heating altitude [these are included in Eq. (8)]. In a nonlinear model, this might appear as low-level convergence generated by downdrafts (Tao and Simpson, 1984);

2) interactions between clouds at different altitudes (no observational support for this);

3) a structured atmosphere allowing trapped horizontally propagating waves;

4) other mechanisms such as direct turbulent entrainment.

An example of this latter mechanism would be the simulations of Wilkins et al. (1976). They found cloud merging in an unstratified fluid (i.e., no gravity waves) but this was clearly due to entrainment of nearby plumes. Most other simulations, and the real atmosphere, have stratification and a rigid lower boundary thus allowing for reflection of wave groups (Malkus, 1954; Simpson, 1980; Orville et al., 1980). Equation (8) can be used to show that with a rigid boundary the heat induced vertical wave motion is much more likely to initiate new convection.

b. Heat island/orographic rain

A downward displacement over a heated island and upward displacement at the downstream side has been observed by Malkus (1963) and Garstang et al. (1975). To explain this, we apply the solution found in section 3 to the heat island problems.

Figure 6 shows the disturbance generated by a stationary heat source (stippled region) introduced at an initial time, $t = 0$, in a hydrostatic atmosphere over a flat surface. The heating represents the low-level heating caused by a heated island in the daytime. For the heating rate, we consider a simple case of a heat island which warms 10°C from 0600 to 1400 LST. For simplicity, we assume that the heating extends uniformly to the top of the planetary boundary layer, say 1 km. The heat flux thus calculated is approximately 348 J m^2 s^{-1}. In Fig. 6, we use a heating rate of 0.35 J kg^{-1} s^{-1} which corresponds to the above heat flux.

The response of the fluid to the low level heating is similar to the case in Fig. 4 in that heating correlates with negative displacement. The dynamics is essentially the same as explained in Section 3. Notice that the air parcel ascends on the downwind side of the heat island.

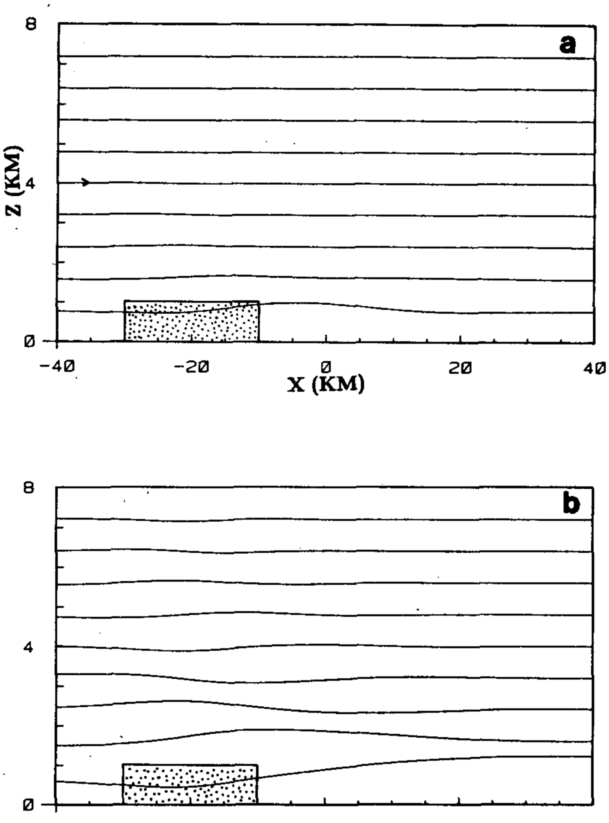

FIG. 6. Vertical displacement for an airflow over a heat island. The stationary heat source is concentrated in the stippled region. This flow is given by Eq. (13) with $U = 5$ m s^{-1}, $N = 0.01$ s^{-1}, $\bar{T} = 273$ K, $Q_0 = 0.35$ J kg^{-1} s^{-1}, $z_0 = 0.5$ km, $b = 10$ km, $d = 0.5$ km and $c = 20$ km. Two times are shown (a) 5000 s and (b) 20 000 s.

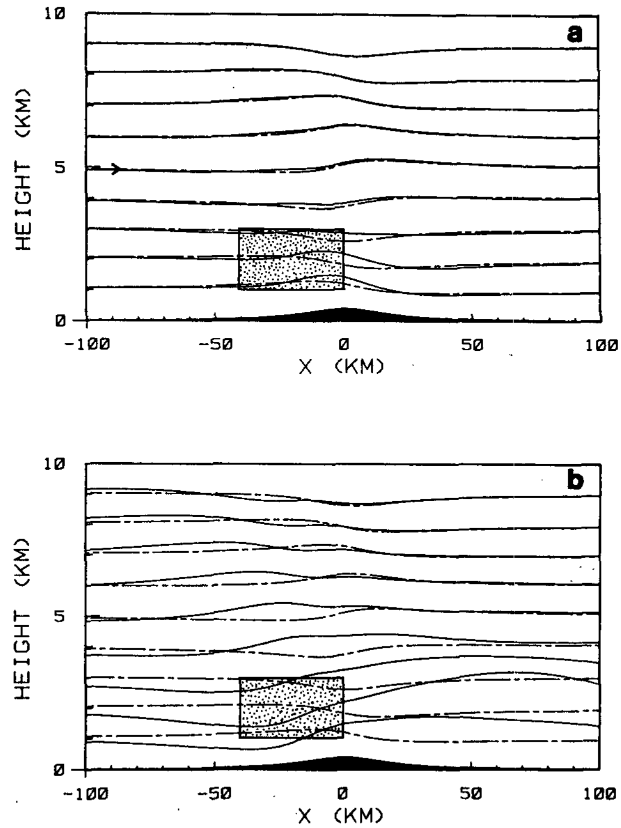

FIG. 7. Vertical displacement generated by a hydrostatic mountain and an elevated heat source (stippled) begun at $t = 0$. The solution is given with $U = 10$ m s^{-1}, $N = 0.01$ s^{-1}, $\bar{T} = 273$ K, $Q_0 = 1$ J kg^{-1} s^{-1}, $b = 20$ km, $d = 1$ km, $c = 20$ km, $a = 20$ km, $h_0 = 400$ m. The dashed lines represent the vertical displacement of the adiabatic mountain waves. Two times are shown in (a) 3000 s, and (b) 13 000 s. The heating corresponds to a precipitation of 2.5 mm h^{-1}.

The observations of rainfall enhancement occurring in the downwind side of the metropolitan area, for example St. Louis (Changnon, 1972), may be partly the result of the ascent produced by the stationary heating of the urban island.

Figure 7 shows an example in which the heating is caused by a stationary precipitating upslope orographic cloud in a hydrostatic atmosphere. This figure is constructed corresponding to a rainfall rate of about 2.5 mm h^{-1}. The heating is concentrated in the stippled region and turned on at $t = 0$ sec. As in the last section, the solution can be obtained by superimposing the dry mountain wave solution with Eq. (13). The dry mountain wave is also plotted for comparison. After some time, the thermally generated displacement has grown and drifted downstream. This displacement keeps growing as the steady heating continues reaching considerable size by 13 000 seconds (Fig. 7b).

If the heating continues for some time, a negative displacement is produced in the vicinity of the stationary heat source (Fig. 7b). This phenomenon was found in SL and more completely explained here. In the real atmosphere, broad upslope rain may be limited by the heat induced descent either in duration or intensity. This result has some similarities to a number of studies of mountain waves and orographic rain (e.g., Raymond, 1972; Fraser et al., 1973; Barcilon et al., 1980).

The vertical transport of the horizontal momentum is convergent at the heating layer, which is similar to the case of an unbounded fluid (Fig. 5) with the modification of orographic effects. With certain realistic values of the parameters U, N, Q_0, b, d, and z_0, a positive momentum flux below the heating layer is produced implying a reverse of the mountain drag as discussed in SL and Durran and Klemp (1982).

c. *Squall-line*

The maintenance of a near steady state squall line remains an unsolved dynamical problem. In the following, we will apply the theory developed in previous section to the low-level flow of a squall line.

One may regard the evaporative cooling in the subcloud layer produced by the precipitation falling from the updraft aloft as a stationary heat sink in the reference frame of the moving line. The steady state assumption of the cooling in a squall-line type of thunderstorm is not an unreasonable one (Lilly, 1979). Figure 8 shows an example of an airflow over a stationary heat sink. In a moving frame, the stationary heat sink may be regarded as a left-moving squall line. The propagation speed of the heat sink is 15 m s^{-1} and the Froude number is 1.5. In the vicinity of the switched on heat sink, the air is displaced downward at first and then upward. The approach to steady state is essentially the same as in the last section except for the upward displacement because of cooling instead of heating. The local features near the heat sink are similar to the steady state solutions of SL and Thorpe et al. (1980). The phase relationship between the evaporative cooling and the induced vertical displacement in the region near the heat sink is negative, as shown earlier. The upstream tilt of the vertical displacement indicates the upward propagation of the generated internal gravity waves. In addition there is a region of positive displacement advecting downstream kinematically, which is similar to the heating case studied earlier.

The positive displacement in the vicinity of the heat sink resembles the flow structure near the front of a squall line and may provide a possible mechanism for the maintenance of a squall line. Robustness of this result can be demonstrated by solving the same problem with a linear numerical model (Lin, 1984). This is also a convenient way to exhibit other aspects of flow field as all of the flow variables are computed by the model. Figure 9 shows that the vertical displacement, the perturbation fields of the density, the horizontal velocity and the vertical velocity at 4000 sec. The field of vertical displacement of the numerical model (Fig. 9a) is slightly smoother than that of the analytical solution (Fig. 8b) because a numerical smoothing technique is applied in the model to avoid the spurious growth of high wave number modes. In general, the agreement of the numerical and analytical results is good. The density field (Fig. 9b) shows that there is a pool of cold air existing near the stationary heat sink. The sharp density difference in front of the heat sink ($x = -35$ km) may be regarded as an upstream gust front produced by the density current. The high density region may correspond to the mesohigh as often observed under the strong downdraft region. On the downwind side, the cold air is advected more dispersively, i.e., the density difference is not as sharp as on the upstream side. From the velocity fields (Fig. 9c, d), there is an upstream motion and a region of surface convergence in front of the stationary heat sink. This is consistent with the finding of the positive displacement near the heat sink (Fig. 8). In application to the low-level flow of a squall line, the upward motion and low-level convergence may play an important role in

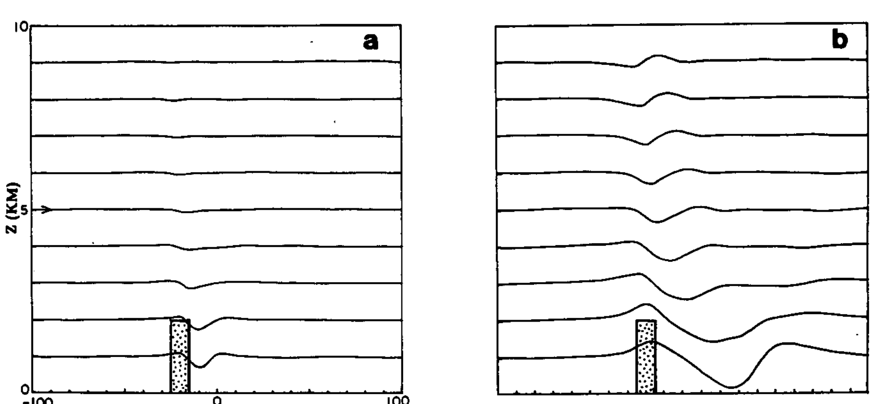

FIG. 8. Vertical displacement near a stationary heat sink representing evaporative cooling under a precipitating cloud. This flow is given by Eq. (13) with $U = 15$ m s^{-1}, $N = 0.01$ s^{-1}, $\bar{T} = 273$ K, $Q_0 = -4$ J kg^{-1} s^{-1}, $z_0 = 1$ km, $b = 5$ km, $d = 1$ km, and $c = 20$ km. Two times are shown in (a) 1000 s, and (b) 4000 s.

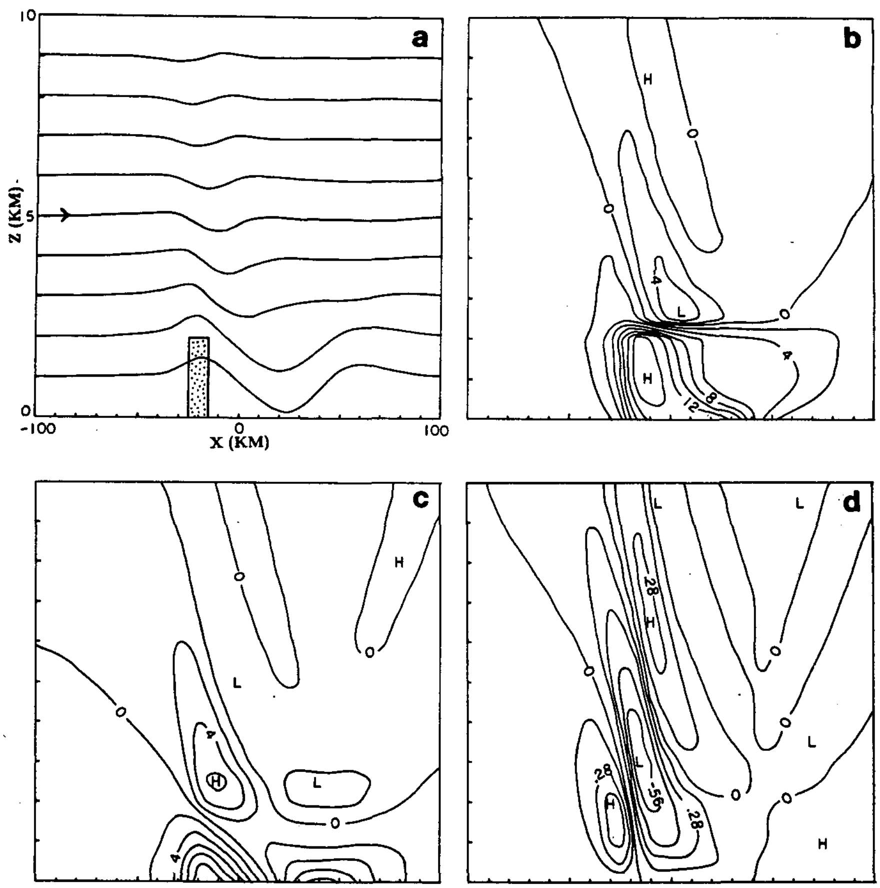

FIG. 9. Airflow near a stationary heat sink simulated by a numerical model at 4000 sec. The parameters are same as that in Fig. 8; (a) vertical displacement, (b) density field, (c) horizontal perturbation velocity, and (d) vertical perturbation velocity.

generating a new convective area on the upstream side of the moving squall line. This may help to explain the maintenance of a squall line which can last for several hours. The limitations of this theory will be discussed in the next section.

5. Concluding remarks

- A time-dependent linearized problem was solved analytically for an airflow over a local heat source. The theory provides an explanation of the negative phase relationship between heating and vertical displacement and the lack of a true steady state noted by other authors.
- The results indicate that the gravity waves generated by the latent heating in cumulus clouds in a region with no boundaries decay too rapidly to form a new merging cloud.
- It was found that air parcels descend over a heat island and ascend on the downwind side. The observed rainfall enhancement occurring on the downwind side of warm metropolitan areas may be partly the result of this effect.
- Broad upslope rain may be limited in duration or intensity by the descent produced by the long-lasting latent heating. However, upslope triggered convection might still persist in the presence of this subsidence. The result offers an explanation for the weakening of mountain waves and orographic clouds in a stable atmosphere as found in other studies.
- The approach to steady state of an airflow near a low-level heat sink involves local positive displacement. There exists upward motion and a region of surface convergence on the upstream side of the heat sink, which might produce a new convective area. This might offer a possible mechanism of the maintenance of a moving squall line.
- The reader should keep in mind that we have neglected the vertical wind shear, nonlinearity, nonhydrostatic effects and have only considered prescribed heating or cooling. The limitations of linear theory for this type of flow have been discussed in Lin (1984). In the real atmosphere, these effects may play an important role for a strong heating or cooling and in, for example, a convective system such as a cumulus cloud or squall line. To study these effects, a more sophisticated model is necessary. To investigate the complete

circulation of a squall line, vertical wind shear (e.g., Thorpe et al., 1982; Seitter and Kuo, 1983) and a more realistic heating and cooling may have to be included in the model. However, the present theory provides valuable qualitative information on the transient effects of an airflow over a local heat source or sink.

Acknowledgments. The authors would like to thank R. Hughes and W. D. Chen of Yale University and D. J. Raymond of New Mexico Tech for their valuable comments on this work. Acknowledgment is made to the National Center for Atmospheric Research (NCAR), which is sponsored by the National Science Foundation, for supporting the computations on CRAY-1. This research is supported by the National Science Foundation Grant ATM-8303632.

REFERENCES

Barcilon, A., J. C. Jusem and S. Blumsack, 1980: Pseudo-adiabatic flow over a two-dimensional ridge. *Geophys. Astrophys. Fluid Dynamics,* **16,** 19–33.

Blumen, W., and R. G. Hendl, 1969: On the role of Joule heating as a source of gravity wave energy above 100 km. *J. Atmos. Sci.,* **26,** 210–217.

Byers, H. R., and R. R. Braham, Jr., 1949: *The Thunderstorm: Report of the Thunderstorm Project.* U.S. Government Printing Office, 287 pp.

Changnon, S. A., 1972: Urban effects on thunderstorm and hailstorm frequencies. *Conf. Urban Environ.,* Philadelphia, Amer. Meteor. Soc.

Dennis, A. S., C. A. Schock and A. Koscielski, 1970: Characteristics of hailstorms of western South Dakota. *J. Appl Meteor.,* **9,** 127–135.

DeSouza, R. L., 1972: A study of atmospheric flow over a tropical island. M.A. thesis, Dept. of Meteor., Florida State University, 203 pp.

Durran, D. R., and J. B. Klemp, 1982: The effects of moisture on trapped mountain lee waves. *J. Atmos. Sci.,* **39,** 2490–2506.

Eliassen, A., and E. Palm, 1960: On the transfer of energy in stationary mountain waves. *Geofys. Publ.,* **22,** 1–23.

Fraser, A. B., R. Easter and P. Hobbs, 1973: A theoretical study of the flow of air and fallout of solid precipitation over mountainous terrain: Part I. Airflow model. *J. Atmos. Sci.,* **30,** 813–823.

Garstang, M., P. D. Tyson and G. D. Emmitt, 1975: The structure of heat islands. *Rev. Geophys. and Space Phys.,* **13,** 139–165.

Hoiland, E., 1951: Fluid flow over a corrugated bed. Appendix A, Fifth Prog. Rep., Contract AF19 (122)-263. Air Force Cambridge Research Center.

Hunt, J. N., R. Palmer and W. Penney, 1960: Atmospheric waves caused by large explosions. *Phil. Trans. Roy. Soc. London,* **A252,** 275–315.

Lilly, D. K., 1979: The dynamical structure and evolution of thunderstorms and squall lines. *Ann. Rev. Earth Planet. Sci.,* **7,** 117–161.

Lin, Y. L., 1984: The dynamics of orographic rain with large latent heat release. Ph.D. dissertation, Yale University, 168 pp.

Malkus, J. S., 1954: Some results of a trade-cumulus cloud investigation. *J. Meteor.,* **11,** 220–237.

——, 1963: Tropical rain induced by a small natural heat source. *J. Appl. Meteor.,* **2,** 547–556.

——, and M. E. Stern, 1953: The flow of a stable atmosphere over a heat island, Part I. *J. Meteor.,* **10,** 30–41.

Olfe, D. B., and R. L. Lee, 1971: Linearized calculation of urban heat island convection effects. *J. Atmos. Sci.,* **28,** 1374–1388.

Orville, H. D., Y.-H. Kuo, R. D. Farley and C. S. Hwang, 1980: Numerical simulation of cloud interactions. *J. Rech. Atmos.,* 499–516.

Palm, E., 1953: On formation of surface waves. *Astrophys. Norvegica,* Vol. V, No. 3, 1–129.

Pekeris, C. L., 1948: The propagation of a pulse in the atmosphere, Part II. *Phys. Rev.,* **73,** 145–154.

Raymond, D. J., 1972: Calculation of airflow over an arbitrary ridge including diabatic heating and cooling. *J. Atmos. Sci.,* **29,** 837–843.

——, 1983: Wave-CISK in mass flux form. *J. Atmos. Sci.,* **40,** 2561–2572.

Queney, P., 1954: Initial value problems in a double Couette-flow. Autobarotropic Flow Project, Sci. Rep. No. 1, Contract AF 19 (604)-728. Air Force Cambridge Research Center.

Scorer, R. S., 1950: The dispersion of a pressure pulse in the atmosphere. *Proc. Roy. Soc. London,* **A201,** 137–157.

Seitter, K. L., and H.-L. Kuo, 1983: The dynamical structure of squall-line type thunderstorm. *J. Atmos. Sci.,* **40,** 2831–2854.

Simpson, J., 1980: Downdrafts as linkages in dynamic cumulus seeding effects. *J. Appl. Meteor.,* **19,** 477–487.

Smith, R. B., and Y. L. Lin, 1982: The addition of heat to a stratified airstream with application to the dynamics of orographic rain. *Quart. J. Roy. Meteor. Soc.,* **108,** 353–378.

Smith, R. C., 1957: Air motion over a heated land mass, II. *Quart. J. Roy. Meteor. Soc.,* **83,** 248–256.

Tao, W.-K., and J. Simpson, 1984: Cloud interactions and merging: Numerical simulations. *J. Atmos. Sci.,* **41,** 2901–2917.

Thorpe, A. J., M. J. Miller and M. W. Moncrieff, 1980: Dynamical models of two-dimensional downdraughts. *Quart. J. Roy. Meteor. Soc.,* **106,** 463–484.

——, —— and ——, 1982: Two-dimensional convection in non-constant shear: A model of mid-latitude squall lines. *Quart. J. Roy. Meteor. Soc.,* **108,** 739–762.

Westcott, N., 1984: A horizontal perspective on cloud mergers. *Bull. Amer. Meteor. Soc.,* **65,** 219–226.

Weston, V. H., 1962: Gravity and acoustical waves. *Can. J. Phys.,* **40,** 446–453.

Wilkins, E. M., Y. K. Sasaki, G. E. Gerber and W. H. Chaplin, Jr., 1976: Numerical simulation of the lateral interactions between buoyant clouds. *J. Atmos. Sci.,* **33,** 1321–1329.